The high resolution infrared spectrum of CH_3D in the region 900 - 1700 cm^{-1}.

A. NIKITIN †, J.P. CHAMPION,

Laboratoire de Physique (Unité associée au C.N.R.S.), Université de Bourgogne, 9 Avenue A. Savary, B.P. 140 - 21011 Dijon, FRANCE

† *Permanent address : Laboratory of Theoretical Spectroscopy, Institute of Atmospheric Optics, Russian Academy of Sciences, 634055 Tomsk, RUSSIA*

VL.G. TYUTEREV

Laboratoire de Spectroscopie Moléculaire Atmosphérique (U.R.A. C.N.R.S. D 1434), Faculté des Sciences, Université de Reims, B.P. 347 - 51623 Reims, FRANCE

ANI)

L.R. BROWN

Jet Propulsion Laboratory, California Institute of Technology, Pasadena, CA 91109 USA.

Abstract

The high resolution absorption spectrum of CH_3D in the region 900 - 1700 cm^{-1} has been revisited on the basis of new long path experimental data recorded with the Fourier transform spectrometer at Kitt Peak. A theoretical model used previously for spherical rotors has been adapted for polyatomic molecules in order to analyze the vibrational polyads of CH_3D simultaneously. Both Triad and Nonad-Triad band systems have been investigated. The hot band intensities were estimated through direct extrapolation of the Triad dipole moments. 600" lines from the hot bands have been assigned and combined with other data for the Triad. The main hot bands contributions are due to $2\nu_6 - \nu_6$, $2\nu_3 - \nu_3$, $\nu_3 + \nu_6 - \nu_3$ and $\nu_3 + \nu_6 - \nu_6$ bands. The standard deviation achieved for 3377 line positions of the Triad was $0.56\,10^{-3}$ cm^{-1}, representing an improvement of one order of magnitude with respect to the most recent analysis.

I.. Introduction

Methane is an important constituent of the planetary atmospheres. Recent works have provided modelized spectroscopic data (successfully modeled line positions and intensities) for the tetrahedral isotopic species $^{12}CH_4$ and $^{13}CH_4$ (*1*) - (*7*), and then predicted line parameters with accuracies close to the requirements of atmospheric applications from the microwave to infrared up to the 3 μm region. However, the analysis of the CH_3D spectrum is incomplete above 2400 cm^{-1}. For example, while the spectroscopic databases like (*8*) or (*9*) contain reasonable predictions for the four fundamentals between 1150 and 2200 cm^{-1}, the 2400 to 3200 cm^{-1} region essentially consists of experimental values measured in natural isotopic abundance which were partially assigned from unpublished work by Olson (see Refs.

(8), (10). The analysis of this upper region is very complex because it involves a set of nine interacting states (the Nonad) shown in Table 1. To facilitate the analysis of this polyad, an extended re-analysis of the lower polyad (ν_3, ν_5, ν_6) has been performed so that Nonad levels could be identified through the hot band transitions in the Nonad - Triad system. The strongest features of the absorption spectrum of CH_3D in the 900 - 1700 cm^{-1} region arise from the three lowest fundamentals (ν_3, ν_5, ν_6). Some 3240 Triad positions and 80 intensities have been previously analyzed by Tarrago et al. (11), (12), (13), (14) with rms values of 0.007 cm^{-1} and 3.4 % respectively. In the present work, some 300 new Triad assignments and 600 transitions from the hot bands have been located. However, the assignment process via the method of combination differences required that the Triad levels be calculated with better accuracies. To accomplish this, the method of vibrational extrapolation used for tetrahedral molecules was adapted to symmetric rotors using the theoretical model described in the previous paper (15).

The exercise validated the theoretical approach and demonstrated that the rovibrational effects within the Triad could be extrapolated to the Nonad states. The present paper reports the results achieved in both Triad and Nonad - Triad systems.

2. Theoretical Framework

An effective Hamiltonian in tensorial form has been used to provide a consistent simultaneous analysis of the lower polyads of the molecule. As described in the previous paper (15), any possible vibration-rotation term is constructed from tensor products of elementary operators.

Rotational operators are given by tensor powers of the standard dimensionless angular moment operators referenced to molecule-fixed axes. Vibrational operators are given by tensor products of creation and annihilation elementary operators associated with the six normal modes of the molecule. Rovibrational operators are then obtained from totally symmetric and hermitian tensor products of the previous operators.

According to the vibrational extrapolation method developed for tetrahedral molecules (6), in the present case, the effective rovibrational hamiltonian adapted to the polyad structure of the CH_3D molecule is expressed as:

$$\mathcal{H} = \mathcal{H}_{\{G.S.\}} + \mathcal{H}_{\{Triad\}} + \mathcal{H}_{\{Nonad\}} + \quad (1)$$

where the subsequent terms correspond to a given polyad.

$$\mathcal{H}_{\{G.S.\}} = \sum t_o^{\Omega(K,\kappa A_1)} T_o^{\Omega(K,\kappa A_1)} \quad (2)$$

contains pure rotational operators (so-called Ground State terms).

$$\mathcal{H}_{\{Triad\}} = \sum t_{b,b'}^{\Omega(K,\kappa\Gamma)CC'} T_{b,b'}^{\Omega(K,\kappa\Gamma)CC'} \quad (3)$$

gathers all $q^2 J^\Omega$ type operators (so-called Triad terms).

Finally $\mathcal{H}_{Nonad}$ gathers all operators (so called Nonad terms) of the type $q^2 J^\Omega$ $q^3 J^\Omega$ and $q^4 J^\Omega$ according to

$$H_{\{Nonad\}} = \sum t_{s,s'}^{\Omega(K,\kappa\Gamma)CC'} T_{s,s'}^{\Omega(K,\kappa\Gamma)CC'} \cdot \sum t_{s,bb'}^{\Omega(K,\kappa\Gamma)CC'} T_{s,bb'}^{\Omega(K,\kappa\Gamma)CC'} + \sum t_{bb',b''b'''}^{\Omega(K,\kappa\Gamma)CC'} T_{bb',b''b'''}^{\Omega(K,\kappa\Gamma)CC'} \cdot \quad (4$$

In the above expressions, Ω is the degree in elementary components J_α, K the tensor rank relative to the space rotation group $O(3)$, κ refers to the projection on the Oz axis, C, C' and Γ designate the symmetry in the point group C_{3v}. s and b refer to stretching and bending modes respectively.

The effective Hamiltonian associated with the subsequent polyads include one, two or three sets of terms obtained by projection of Eq(1) on the corresponding subspaces

$$H^{<G.S.>} = H_{\{G.S.\}}^{<G.S.>} \quad (5)$$

$$H^{<Triad>} = H_{\{G.S.\}}^{<Triad>} + H_{\{Triad\}}^{<Triad>} \quad (6)$$

$$H^{<Nonad>} = H_{\{G.S.\}}^{<Nonad>} + H_{\{Triad\}}^{<Nonad>} \cdot H_{\{Nonad\}}^{<Nonad>} \quad (7)$$

The dipolar transition moment is similarly expressed in tensorial form. It is partially transformed according to the polyad pattern of the CH_3D molecule. In the present work both Triad - G.S. and Nonad - Triad systems are considered. The corresponding transition moments are formally expressed as

$$M^{<GS,Triad>} = M_{\{G.S.\},\{Triad\}}^{<GS,Triad>} \quad (8)$$

$$M^{<Triad,Nonad>} = M_{\{G.S.\},\{Triad\}}^{<Triad,Nonad>} + M_{\{Triad\},\{Nonad\}}^{<Triad,Nonad>} \quad (9)$$

The lower order terms are the same in the above two expressions. It means that, at first approximation, the transition moments of the Nonad - Triad system can be estimated from the intensity analysis of the Triad - GS band system.

In the present work, the successive terms of the Hamiltonian expansion (1) have been developed to the order 6,4 and 4 respectively in the Amat-Nielsen classification scheme (*16*). The corresponding numbers of symmetry allowed terms is 13, 89 and 474. The dipolar transition moment was developed to the 0-th order including 3 terms.

3. Experimenta Details

The experimental data used in the present study have two origins:

1 - Data from the FTS of Laboratoire d'Infrarouge reported in (*13*) and included in the HITRAN and GEISA Databases. Among the 3495 transitions listed in (*11*) up to $J = 18$ (measured line positions and calculated line intensities) we used 3240 transitions only. The remaining transitions were not included in our fit because they were subject to experimental inaccuracy (weak line on the wing of stronger line, discrepancy with respect to

our new experimental measurements, strongly asymmetric line profile ...). In addition, the upper energy levels derived from such rejected lines generally had large deviations from the corresponding average values calculated from other partner transitions.

2 - Scans recorded at Kitt Peak with long path lengths (Table 2).

Laboratory spectra of CH_3D were recorded at 0.0054 and 0.012 cm-1 resolution with the McMath Fourier transform spectrometer located at Kitt Peak National Observatory/ National Solar Observatory near Tucson, AR. The spectra for the Triad region were obtained using a KCl beamsplitter and helium-cooled Ar-doped Si detectors while the spectra for the Nonad region were recorded with the CaF2 beamsplitter and In-Sn detectors. As seen in Table 2, five different absorption cells were used. A 6-m base multipass chamber was employed to achieve long path required to observe hot band lines. Signal to noise ratios of 300:1 or better were generally obtained with integration times of 70 minutes. To calibrate the line positions, CO or OCS was placed in a second chamber in line with the cell containing the CH_3D. Residual water lines were also used. Line centers were found by using the peaklist program of the AirSentry project (*17*) and by least squares curve-fitting of the unapodized spectrum (*18*). The rms of the calibration line centers of CO and OCS was 0.00005 cm-1 or better. However, because of the complexity of the high density spectrum, the precision of a CH_3D line center for a strong well isolated feature was thought to be somewhat worse.

To assign the 900 new lines by combination differences, a quantitative criterion was used to select transitions involving each Triad level in order to obtain an averaged experimental energy assuming the ground state energies were accurately known. The standard deviation on the resulting combination differences were 0.25 10^{-3} cm^{-1} for 3317 transitions. This value represents an estimate of the relative accuracy of the data fitted.

4. Analysis of the Triad

The first step of the present work was to convert the results of the previous analysis (*12*), (*13*) into our tensorial model. Ground State parameters were taken from (*13*) and converted using the relations given in (*19*), (*15*). No refinement of the ground state constants was attempted since combination differences on our new data was found quite consistent with experimental accuracy (see previous section). The Triad parameters of (*11*), (*13*) were used as initial parameters for our nonlinear least-squares fit. The main parameters were calculated using the relations given in (*15*). We checked both the theoretical relationships and computer programs by reproducing the calculations of (*11*), (*13*) within the computer accuracy for the Ground State. Then we performed iterative fitting of the assignments mentioned above. Our best fit includes 42 Triad parameters adjusted on 3377 transitions up to $J = 18$ including practically all possible values of K up to $K = 17$ for the three bands. The overall standard deviation was 0.56 1 0^{-3} 0//"] (0.60 cm^{-1} for ν_3, 0.52 cm^{-1} for ν_5, ().57 cm^{-1} for ν_6). Table 3 gives the values of the 42 adjusted parameters (Ground State parameters were kept fixed). As seen in the last column of Table 3, which gives the classical terms involved in our tensorial operators, the model applied for the Triad includes all the diagonal quartic terms, eight Coriolis terms, nine anharmonic terms plus three terms (# 50, 54 and 69) not considered in the prior studies. We have not converted our tensorial parameters into the classical spectroscopic constants because our prediction would not be reproduced if these new terms were omitted. Note that the diagonal Triad terms denoted by $\wedge$ represent vibrational dependencies of the corresponding ground state values.

The improvement of one Order of magnitude for the standard deviation on the positions with respect to the previous analysis can be explained by several reasons: (i) a few wrong assignments have been eliminated (ii) blended transitions have been removed from the fit (iii) all group theoretically allowed terms was systematically considered using our algorithms. Note that a sensible improvement would certainly have been obtained using the new set of data with the model of the previous analysis. However, the new terms considered here proved to be significant. The remaining discrepancy between the standard deviation achieved and the experimental precision estimated from combination differences suggests that higher order terms should be added. Such an extension would require a detailled study of the ambiguities of the effective Hamiltonian which was not in the scope of the present paper. To calculate line intensities, we repeated the fit of the 80 measurements of Ref. (*14*) in order to get intensity parameters consistent with our present eigenfunctions. The values of the corresponding dipole moments to the same order of approximation in tensor form are listed in Table 4. We have not converted our tensorial parameters into the classical constants for the same reason as for Hamiltonian parameters. The standard deviation obtained on the 80 data was 3.8%. Despite the fact that our model gives a more systematic description of first order perturbation effects than the empirical Herman-Wallis constants, this value is slightly larger than the value of the prior results. This is probably because, unlike in the prior results, in our fit all data were given the same weight.

Table 5 lists transitions near 1154 cm^{-1}, showing the observed position, calculated intensity, observed - calculated position and quantum assignment. Figure 1 illustrates the quality of the Triad analysis by showing the observed and calculated spectra in the region of the ν_6 Q branch at 1145 cm^{-1}. The residual differences in percent are plotted along the bottom." The observed data is the first spectrum listed in Table 1.

5. Assignment of the hot band system Nonad - Triad

After the new study of the Triad was completed, the line positions and intensities of the Nonad Triad system were predicted. The parameters for the Nonad upper state levels were taken from preliminary analyses of the 3 to 5 μm spectra using the model defined by Eq. (1). This latter work is to be reported in a subsequent paper. The hot band intensities were estimated through direct extrapolation of the Triad dipole moments as follows. We used the first order parameters involved in the Triad-GS part of Eqs. (8 and 9) determined from the fit of the 80 measurements of the Triad mentioned in the preceding Section (parameter values quoted in Table 5). This set of parameters provide an estimate of the Nonad - Triad hot band intensity good to the zero-th order of approximation only since there exist 11 first order extra parameters in the Nonad-Triad part of Eq 9 that were not considered. These omitted terms are pure vibrational terms connecting the Triad to the fundamental states of the Nonad. Table 6 lists summations of the predicted line intensities for 24 hot bands involving seven of the Nonad upper states. For the reasons mentioned above, the sums reported in Table 6 should not be considered as the true integrated band strengths, but they do provide some indication of the band intensities. In fact, from visual inspection of the spectra, we found a satisfying agreement between the predicted hot line intensities and the observed ones. As seen in Table 6, the strongest hot bands are predicted to be $2\nu_6(E + A_1)$ ν_6, $\nu_3 + \nu_6$ ν_6, $\nu_3 + \nu_6 - \nu_3$ and $2\nu_3 - \nu_3$, and most of the 600 assigned hot band lines belong to these bands. A sample of low J identifications are shown in Table 7. Additional effort will be made to extend the hot band analysis as part of the Nonad study

6. Conclusion

The present analysis represents the first step of a global description of the infrared spectrum of the! CH_3D molecule. The theoretical model was chosen to match the polyad structure of the molecule. The tensorial formalism was implemented using new algorithms especially adapted to the simultaneous analysis of complex polyads of polyatomic molecules. New experimental measurements have been reported and used in complement of already published data.

The results achieved in the present work include several aspects: (i) The accuracy of the fit of the Triad transition frequencies has been improved by one order of magnitude with respect to the most recent study; (ii) The corresponding set of Hamiltonian terms provides a good description of the rovibrational interactions among the bending modes of the molecule, directly extrapolable to upper polyads; (iii) Many transitions of the Nonad - Triad system have been predicted and identified. They have significant contributions in the $7\mu m$ region and provide useful informations on the Nonad upper levels. The first comprehensive analysis of the Nonad system is in progress, and will be reported in a subsequent paper.

Acknowledgments

Support for the Dijon laboratory computer equipment from the Région Bourgogne is gratefully acknowledged. The authors thank G.Tarrago and M.Delaveau for making their computer files available. Part of the research reported in this paper was performed at the Jet Propulsion Laboratory, California Institute of Technology, under contract with the National Aeronautics and Space Administration. The authors wish to thank the Kitt Peak National Observatory National Solar Observatory for the use of the FTS and C. Plymate and .1. Wagner for assistance in obtaining the CH_3D spectra.

References

(*1*) L.R .BROWN, J.S.MARGOLIS, J.P. C HAMPION, J.C.HILICO, J.M.JOUVARD, M.LOETE, C.CHACKERIAN JR, G.TARRAGO, AND D.CHRIS BENNER , *J. Quant. Spectrosc. Rad. Transfer* **48**, 617-628 (1 992).

(*2*) J.P.CHAMPION , *Can.J.Phys* **55** , 1802- 182?8 (1977).

(*3*) J.P. CHAMPION, AND G.PIERRE , *J.Mol.Spectrosc.* **79** , 255-280 (1980).

(*4*) J.P.CHAMPION, J.C.HILICO, AN D L.R.BROWN , *J.Mol.Spectrosc.***1** *33, 244-255* (1 989).

(*5*) J.C.HILICO, J.]', CHAMPION, S.TOUMI, VL. G.TY UTE REV, AND S.A.TASHKUN , *J. Mol. Spectrosc.* **168** , 455 476 (1994).

(*6*) J.-P. CHAMPION, M. LOETE, AND G. PIERRE , *in* "Spectroscopy of the Earth's Atmosphere and Interstellar Medium," (K. NARAHARI RAO *and* A. WEBER *Eds)* **pp. 388 397**, Academic Press, Boston, 1992.

(') B.-I. ZHILINSKII, V-I. P EREVALOV, AND VL.-G. TYUTEREV , "Method of In (due.iblc Tensorial Operators in the Theory of Molecular Spect ra, " *(in Russian)* **Nauka**, Novosibirsk. 1987.

(*8*) L. S. ROTHMAN, R.R .GAMACHE, R.H.TIPPING , C.P.RINSLAND, M.A.H.SMITH, D. CHRIS BENNER, V. MATATH Y DEVI, J.-M. FLAUD, C.CAMY-PEYRET, A.PERIN, A. GOLDMAN, S.T. MASSIE, L.R .BROWN, AND R .A.TOTH , J. *Qua nt. Spect rosc. Ra d. Transfer* **48**, No. 5/6 , p.469 507 (1992)

(*9*) N. HUSSON, B. BOUNET, N.A.SCOTT, AND A.CHEDIN , *J. Quant. Spectrosc. Rad. Transfer 48,* No. 5/6 , p.506-518 (1992)

(*10*) W. B. OLSON , *J. Mol. Spectrosc.* **43**, 190-198 (1972)

(11) M. DELAVEAU , *Thesis* **Orsay France**, (1 98 s).

(*12*) G. TARRAGO, AND M. DELAVEAU , *J. Mol. Spectrosc.* **119** , 418-425 (1986).

(*13*) G.TARRAGO, M. D ELAVEAU, L. FUSINA, AND G. GUELACHVILI , J. *Mol.Spectrosc.* **126** , 149-158 (19s7).

(*14*) G. TARRAGO, G . RESTELLI, AND F. CAPPELLANI , J. *Mol. Spectrosc. 129*) 326332 *(1* 988).

(*15*) A. NIKITIN, J .-P. CHAMPION, AND VL.-G. TYUTEREV , , in press J. Mol. Spectrosc. (1 996 or 1997).

(*16*) G. AMAT, H.H. NIELSEN, AND G. TARRAGO, *"Rotation-vibration of polyatomic molecules"* , M. DEKKER, New York (1971).

(*17*) V.F.GOLOVKO, A .V.NIKITIN, A .A.CHURSIN, AN I) VL.G.TYUTEREV , *Databases and Information Syst ems* vol. **2** , Phasis Publishing House , (Moscow, June *27-30,* 1995), pp. *12-14.*

(*18*) L. S. BROWN, J. S. MARGOLIS, R. H. NORTON, AND B. D. STEDRY, *Appl. Spectrosc.* 37, 287-292 (1983)

(*19*) CH. ROCHE, *Thesis* Dijon France, (1994).

Table I . Vibrational Energies of the Triad and Nonad of CH_3D.

Band	Symmetry	Center cm^{-1} (J= ( ))	Ident Numb
ν_6	1<	1161.1030	2
ν_3	$A1$	1306.8478	3
ν_5	E	1472.0234	4
ν_2	A_1	2200.0367	(i
$2\nu_6$	A_1	2316.2765	17
$2\nu_6$	E	2323.2953	16
$\nu_3 + \nu_6$	E	2465.4635	9
$2\nu_3$	A_1	2597.6808	7
$\nu_5 + \nu_6$	E	2623.4389	15
$\nu_5 + \nu_6$	A_1	2633.1592	13
$\nu_5 + \nu_6$	A_2	2634 .8333	14
$\nu_3 + \nu_5$	E	2776.2862	8
$2\nu_5$	A_1	2910.1146	12
$2\nu_5$	E	2940.0985	11
ν_1	A_1	2969.5166	5
ν_4	E	301 6.7089	10

Table 2. Conditions of the Kitt Peak experiments.

Min cm^{-1}	Max cm^{-1}	'T'T'('ss111'(' Torr	Path meter	Tempature K	Resolution cm^{-1}	Calibration
600.	1400."	44.3	().05	293.5	0.0056	OCS
950.	2750.	1.31	25.0	296.2	().0054	H_2O
950.	2750.	1.31	97.0	296.4	0.0054	H_2O
950.	2750.	1.31	385.	296.2	().0054	H_2O
950.	2750.	0.13	25.()	296.0	0.0054	1-0 CO
1800. -	5500.	4.88	0.05	291.0	0.0118	
1800.	5500.	4.88	2.39	291.0	0.0118	2-o CO
1800.	5500.	().72	2.39	291.0	0.0118	
1800.	Moo.	89.6	1.50	295.6	().010{)	1-0 CO

Table 3. Effective 11 amiltonian parameters for the Triad of CH_3D.

Nomenclature			
Rotational	Vibrational	Parameter value	Notation (12)
		Ground State constants	
1 R2(0,0A1)	"000000000000	4.3370 50770	A ; B
2 R2(2,0A1)	000000000000	0.2797663647	A ; B
3 R4(0,0A1j	000000000000	-7.89402s 10^{-5}	D^J ; D^{JK} & D^{KK}
4 R4(2,0A1)	000000000000	5.188416 10-(	D^{JK} ; D^{KK}
5 R4(4,0A1)	000000000000	2.35601510^{-6}	D^{KK}
(i R6(0,0A1)	000000000000	3.74800010-<"	H^J ; H^{JJK}; H^{JKK} ; H^K
7 R6(2,0A1)	000000 000000	1,940455 10^{-10}	H^{JJK} ; H^{JKK} ; H^K
8 R6(4,0A1)	000000000000"	1.036627 10-^{10}	H^{JKK} ; H^K
9 R6(6,0A1)	)00000000	-4.317880 10^{-12}	H^K
		Diagonal ν_3 terms	
10 R0(0,0A1)	001000001000	1306.847852(44)	ν
11 R2(0,0A1)	001000001000	-6.961712(45)10^{-2}	$\wedge A$; $\wedge B$
12 R2(2,0A1)	001000001000"	1.222042(17) 10^{-2}	$\wedge A$; $\wedge B$
13 R4(0,0A1)	001000001000	3.291(49) 10^{-7}	$A\ l\ )'$; $\wedge D^{JK}$; $\wedge D^{KK}$
14 R4(2,0A1)	001000001000"	3.636(11)10^{-7}	$\wedge D^{JK}$; $\wedge D^{KK}$
15 R4(4,0A1)	001000001000	-1.3889(39) 10^{-7}	$\wedge D^{KK}$
		$\nu_3 <$ - $>$ ν_5 interaction terms	
17 R1 (1,1E)	001000 00001 0	-4.10099 21(79)	C_{11}^1
18 R2(2,1E)	001000000010 0		
19 R2(2,2E)	OOJOOOOOOO10 ()		
20 R3(1,1E)	001000000010	-2.01729(46) 10^{-4}	C_{11}^{3a} ; C_{11}^{3b}
21 R3(3,1E)	001000000010	4."/947(28) 10^{-5}	C_{11}^{3b}
22 R3(3,2E)	001000000010 0		
		$\nu_3 <$ - $> \nu_6$ interaction terms	
28 R1(1,1E)	6 0 1 0 0 0 0 0 0 6 0 1	2.4372543(99)	C_{11}^1
29 R2(2,1,11;)	001000000001	-6.81284(74) 10^{-3}	C_{11}^2
30 R2(2,2E)	001000000001 0		
31 R3(1 ,1E)	001000000001	7.5944(60) 10^{-5}	C_{11}^{3a} ; C_{11}^{3b}
32 1{.3(3,11';)	001000000001 0		
33 R3(3,2E)	001000000001 0		

Diagonal ν_5 terms

39	1{o(oIOA 1)	00001 O 000010 14 72.023447(52)	ν
40	R1(1,0A2)	000010000010 1 .9138 s84(35)	$A_{\zeta t}$
41	R2(0,0A1)	000010000010 -3.74390(54) 10^{-3}	$\wedge A$; $\wedge B$
42	R2(2,0A1)	000010000010 -1.869123(30) 10^{-2}	$\wedge A$; $\wedge B$
43	1{2(2,111)	000010000010 3.18871(20) 10^{-2}	q_{12}
44	1{2(2,21!)	000010000010 62465(17) 10^{-3}	q_{22}
45	R3(1,0A2)	000010000010 0	
46	R3(3,0A2)	000010000010 -7.0846(18) 10^{-5}	η_t^K
47	R3(3,3A2)	000010000010 0	
48	R4(0,0A1)	000010000010 -2.3579(59) 10^{-6}	$A1)^{"}$; $\wedge D^{JK}$; $\wedge D^{KK}$
49	R4(2,0A1)	OOOO1O 000010 -4.595(15) 10-"7	$\wedge D^{JK}$; $\wedge D^{KK}$
50	R4(2,1E)	000010000010 9.025(89) 10-7	
52	R4(4,0A1)	000010000010 3.365(13) 10^{-7}	$\wedge D^{KK}$
54	R4(4,1E)	0000]0000010 2.608(53) 10-7	

ν_5 < > ν_6 interaction terms

57	R0(0,0A1)	000010060001 0	
58	R1(1,0A2)	000010000001 1.591202(24)	F^1_{011}
59	1/1(1,11!)	000010000001 3.55 8019(44)	F^1_{111}
60	R2(0,0A1)	000010000001 3.8550(23) 10-^{3}	F^2_{011J} ; F^2_{011K}
61	R2(2,0A1)	000010000001 0	
62	1{2(2,1 E)	000010000001 0	
63	R2(2,2E)	000010000001 3.35602(72) 10^{-2}	F^2_{21},
64	1{3(1 ,0A2)	000010000001 0	
65	1{3(1 ,114:)	000010000001 0	
66	R3(3,3A1)	000010000001 5.4705(85) JO-^{5}	F^3_{311A} ; F^3_{311B}
67	R3(3,0A2)	000010000001 0	
68	R3(3,3A2)	000010000001 -6.406(91) 10^{-6}	F^3_{311A} ; F^3_{311B}
69	R3(3,1E)	000010000001 5.625(12) 10^{-5}	
.70	1{3(3,21':)	000010000001 0	

Diagonal ν_6 terms

81	R0(0,0A1)	000001 000001 1I6I.103O4O(7S)	ν
82	R1(1,0A2)	000001 000001 -4 .400'/081 (82)	$A_{\zeta t}$
s3	R2(0,0A1)	000001 000001 7.3253(47) 10^{-3}	$\wedge A$; $\wedge B$
84	R2(2,0A1)	000001 000001 1.10982(60) 10-^{2}	$\wedge A$; $\wedge B$
85	R2(2,1E)	000001 000001 -3.1153(57) 10-^{2}	q_{12}
86	1{2(2,21':)	000001 000001 1.5116(94) 10-^{2}	q_{22}
87	R3(1,0A2)	000001 000001 -1.8809(19) 10^{-4}	η_t^J ; η_t^K
88	R3(3,0A2)	000001 000001 -4.559(55) 10^{-5}	η_t^K
89	R3(3,3A2)	000001 000001 0	
90	R4(0,0A1)	000001 000001 -3.8'2(13) '10-^{7}	$\wedge D^J$; $\wedge D^{JK}$; $\wedge D^{KK}$
91	R4(2,0A1)	000001 000001 5.123(67) 10"-^{7}	$\wedge D^{JK}$; $\wedge D^{KK}$
94	R4(4,0A 1)_	000001 000001 -1.186([)8) 10-^{7}	$\wedge D^{KK}$

Table 4. Effective Transition Moment Parameters.

Nomenclature				
Rotational	Vibrational		Parameter value	Physical Meaning
1 1{0(0,0/4,)	000000001000	A_1	1.83 10^{-2}	μ_3
2 R0(0,0A_1)	000000000010	E	-1.97 10^{-2}	μ_5
3 R0(0,0A_1)	*000000000001*	E	4.52 10-^{2}	μ_6
4 R1(1,1E)	000000" ()()0()10	A_1	0.0	First Order
5 R1(1,1E)	000000"000001	*Al*	1.2 10-4	Rotational
6 1{1(1 ,11':)	000000 001000	E	0.0	Corrections
7 R1(1,0A_2)	000000000010	E	'2.4 10^{4}	"
s R1(1,1E)	000000000010"	E	0.0	
9 R1(1,0A_2)	*000000* ()()()001	E	0.0	
10 R1(1,1E)	000000000001	E	0.0	"

Table 5. Sample of the Obs-Calc comparison of the IR spectrum of CH_3D

(a)	(b)	(c)	(d)	(e)	(f) V J K C	V'J' K'C'
1153.0109	1.84E-24	652.7794	-0.52	-3	1 12 6 A1	4 1 1 8 A 2
1153,1109	3.17E-22	1182.4530	-0.04	6	1 17 0 A2	4 17 1 Al
1153.1703	6.31E-23	284.5494	0.50	0	1 8 2 E	4 8 0 E
1153.3363	2.38E-23	1579.3286	-8.72	hot,	2 8 0 A I	9 8 1 A2
1153.4633	2.83E-23	1518.7508	-4.45	hot	2 7 0 A2	9 7 1 A1
1153.4792	5.67E-22	105.1 .5484	-0.11		1 16 0 A1	4 16 1 A2
1153.5866	5.67E-23	222.5817	-0.47	0	1 7 2 E	4 7 0 E
1153.6172	3.06E-22	1183.7861	-0.21	4	1 17 1 E	4 17 0 E
1153,7800	1.56E-22	426.1866	-0.46	-2	I 1 O O A 1	4 1 0 4 A 2
1153.82?29	9.74E-22	928.2355	-0.07	1	1 15 0 A2	4 15 1 Al
1153.8689	1.59E-22	813.8782	-0.84	0	1 14 1 E	4 14 5 E
1154.0569	5.43E-22	1052.8856	-0.95	0	1 16 1 E	4 16 0 E
1154.1427	1.60E-21	812.5335	-0.06	0	1 14 0 A1	4 14 1 A2
1154.1614	9.43E-23	1187.7864	-0.24	9	1 17 2 E	4 17 6 E
1154.3017	5.60E-23	1191.7544	-0.21	hot	4 2 1 E	16 2 0 E
1154.4245	2.20E-22	1182.4530	0.51	4	1 17 0 A2	2 16 0 A1
1154.4395	2.53E-21	704.4611	0.07	-1	1 13 0 A2	4 13 1 Al
1154.4903	9.13E-22	929.5"[65	-0.01	0	1 15 1 E	4 15 0 E
1154.5326	2.18E-22	1183.7861	0.89	5	1 17 1 E	2 16 1 E
1154.5329	1.45E-22	1326.2448	-0.11	4	1 18 2 E	4 18 1 E
1154.6398	5.07E-23	1429.0613	-0.21	-4	1 18 9 A1	2 17 9 A2
1154.7137	3.82E-21	604.0352	-0.01	-2	1 12 0 A1	4 12 1 A2
1154.8556	2.12E-22	1187.7864	0.24	4	1 17 2 E	2 16 2 E
1154.9114	4.16E-23	1600.6448	-2.31	hot	4 10 2 A1	16 10 1 A2
1154.9424	1.38E-21	813.8"(82	-0.17	-4	1 14 1 E	4 14 0 E
1154,9663	5.52E-21	511.2?"/22	-0.20	-3	1 11 0 A2	4 11 1 A1
1155.0379	5.55E-23	1506.9886	5.65	hot	4 9 0 E	17 9 1 E
1155.0707	1.77E-21	705.8092	-0.12	5	1 13 1 E	4 13 0 E
1155.1545	5.31E-23	1524.1429	-0.45	hot	4 9 2 A1	16 9 1 A2
1155.1995	7.57E-21	426.1866	-0.16	-3	1 10 0 A1	4 10 1 A2
1155.2457	5.27E-23	1524,0302	0.50	hot	4 9 2 A2	16 9 1 Al
1155.3544	2.03E-22	1194.4567	0.'(2	10	1 17 3 A2	2 16 3 A1
)155.4223	9.50E-21	348.7923	-0.05	-5	1 9 0 A 2	4 9 1 A1
1155.4416	2.03E-22	1194.4567	-0.82	-4	1 17 3 Al	2 16 3 A2
1155.4532	1.41E-22	1332.8936	0.08	*	1 18 3 A2	4 18 2 A1
1155.5217	1.09E-20	279.1018	-0.44	0	1 8 0 A I	4 8 1 A 2
1155.5941	3.48E-21	605.3865	0.01	1	1 12 1 E	4 12 0 E
1155.6861	6.30E-22	705.8092	-0.49	-9	1 13 1 E	4 13 5 E
1155.7286	1.52E-20	217.1261	-0.22	-2	1 7 0 A2	4 7 1 A1
1155.8321	1.93E-21	279,1018	-0.32	-7	1 8 0 A1	4 8 4 A 2
1155.8792	1.73E-20	162.8'/54	-0.20	-3	1 6 0 A1	4 6 1 A 2
1155.9"763	7.04E-23	1393,7864	1.60	-3	4 7 2 A2	16 7 1 A1

1156.0049	1.84E-20	116.3585	--0.07	0	1	5	0	A2	4	5	1	A1
1156.0140	5.03E-21	512.6264	-0.38	4	1	11	1	E	4	11	0	E
1156.0295	8.33E-22	933.6006	0.04	-3	1	15	2	E	4	15	1	E
1156.1084	1.82E-20	77.5828	-0.18	2	1	4	0	A1	4	4	1	A2
1156.1509	1.90E-22	1203.8015	0.81	-3	1	17	4	E	2	16	4	E
1156.1909	1.65E-20	46.5547	-0.14	-3	1	3	0	A2	4	3	1	A1
1156.2525	1.32E-20	23.2792	--0.21	-3	1	2	0	A1	4	2	1	A2
1156.2937	8.54E-21	7.7601	-0.04	3	1	1	0	A2	4	1	1	A1
1156.3368	2.74E-23	1513.8573	-0.22	0	1	18	12	A1	2	17	12	A2
1156.42?42	6.78E-21	427.5436	--0.02	-6	1	10	1	E	4	10	0	E
1156.4874	3.49E-24	770.7004	-0.45	-5	1	13	7	E	4	1	2	9	E
1156.5862	1.19E-22	217.1261	-0.19	-4	1	7	0	A2	4	7	4	Al
1156.62597	.81E-23	1056.8982	--0.45		1	16	2	E	4	16	6	E
1156.6587	1.37E-21	817.9132	0.02	hot	1	14	2	E	4	14	1	E
1156.71147	.21E-23	1294.2077	--3.04	hot	4	5	2	A1	16	5	1	A2
1156.8368	8.63E-21	350.1518	-0.06	O	1	9	1	E	4	9	0	E
1156.96159	.32E-23	605.3865	-0.55	-7	1	12	1	E	4	12	5	E

Table 6. Estimated intensity summations Of the Nonad - Triad System.

Band	#lines	Minimum cm^{-1}	Maximum cm^{-1}	Intensity summation cm/molecule
$\nu_1 - \nu_5$	90	1379	1568	$3\ 10^{-23}$
$2\nu_3 - \nu_3$	320	1100	1382	$4\ 10^{-21}$
$2\nu_3 - \nu_5$	169	1059	1231	$1\ 10^{-22}$
$2\nu_3 - \nu_6$	228	1190	1600	$1\ 10^{-22}$
$\nu_3 + \nu_5 - \nu_3$	488	1304	1622	$6\ 10^{-22}$
$\nu_3 + \nu_5 - \nu_5$	710	1091	1397	$2\ 10^{-21}$
$\nu_3 + \nu_5 - \nu_6$	16	1534	1635	$4\ 10^{-24}$
$\nu_3 + \nu_6 - \nu_3$	645	1032	1373	$4\ 10^{-21}$
$\nu_3 + \nu_6 - \nu_5$	6	1094	1201	$6\ 10^{-25}$
$\nu_3 + \nu_6 - \nu_6$	720	1070	1570	$9\ 10^{-21}$
$\nu_4 - \nu_5$	31	1500	1655	$6\ 10^{-24}$
$2\nu_5(E) - \nu_5$	583	1310	1608	$5\ 10^{-22}$
$2\nu_5(A_1) - \nu_5$	416	1288	1588	$3\ 10^{-22}$
$\nu_5 + \nu_6(A_1) - \nu_3$	79	1191	1424	$6\ 10^{-23}$
$\nu_5 + \nu_6(A_1) - \nu_5$	250	1033	1380	$4\ 10^{-22}$
$\nu_5 + \nu_6(A_1) - \nu_6$	233	1356	1629	$5\ 10^{-22}$
$\nu_5 + \nu_6(A_2) - \nu_3$	126	1176	1390	$9\ 10^{-23}$
$\nu_5 + \nu_6(A_2) - \nu_5$	485	1030	1385	$1\ 10^{-21}$
$\nu_5 + \nu_6(A_2) - \nu_6$	563	1308	1620	$9\ 10^{-22}$
$\nu_5 + \nu_6(E) - \nu_3$	334	1108	1405	$3\ 10^{-22}$
$\nu_5 + \nu_6(E) - \nu_5$	921	1026	1321	$2\ 10^{-21}$
$\nu_5 + \nu_6(E) - \nu_6$	1012	1287	1610	$1\ 10^{-21}$
$2\nu_6(E) - \nu_3$	38	1080	1350	$2\ 10^{-23}$
$2\nu_6(E) - \nu_6$	1141	1021	1396	$1\ 10^{-20}$
$2\nu_6(A_1) - \nu_6$	715	1032	1371	$7\ 10^{-21}$

Table 7. Sample of the Nonad - Triad hot transitions.

(a)	(b)	(c)			(d)	(e)
		V K J C	N	V'K'J' C'	N'	i i'
12?83.2?731	1.5E-23	4 1 1 A2	2	7 0 0 A 1	3 0.02	2 1
1296.6906	1.5E-23	4 0 1 E	1	9 0 0 E	2 -0.88	2 1
12?88.7617	2.1E-23	4 1 2 A 2	1	9 1 1 A1	2 0.41	1 1
1144.7664	2.8E-23	4 1 2 A1	1	17 0 1 A2	2 0.21	2 2
1275.5766	2.8E-23	2 0 2 A1	3	7 0 1 A ?	5 0.09	2 2
1151 .0861	2.9E-23	4 0 1 E	1	16 1 1 E	2 0.47	2 1
1135.7476	8.7E-24	4 0 2 E	2	16 1 1 E	2 0.66	2 1
1288.8266	2.8E-23	4 0 2 E	2	9 0 1 E	5 -0.05	2 2
1141.9064	6.8E-24	2 1 2 E	4	9 0 1 E	5 0.20	3 2
1289.0075	2.0E-23	4 1 2 E	3	9 1 1 E	6 -0.30	1 1
1275.6215	2.0E-23	2 1 2 E	4	7 1 1 E	7 -0.2?8	3 1
1159.5629	5.2E-23	4 1 2 A2	1	17 0 2 A1	3 -0.13	1 2
1137.1863	3.1E-23	4 1 3 A2	1	17 0 2 Al	3 0.00	2 2
1319.0426	2.3E-23	4 1 1 A2	1	9 1 2 A1	5 -0.73	2 2
1281.0484	3.4E--23	4 1 3 A2	1	9 1 2 A1	5 -0.29	2 2
1267."/'470	3.7E--23	2 0 3 A 2	3	7 0 2 A1	7 0.38	2 1
131906453	5.0E-24	3 1 1 A2	3	8 1 2 A1	12 -0.10	2 2
1319.3375	2.3E-23	4 1 1 A1	1	9 1 2 A2	3 -0.13	1 1
1319.6126	5.1E-24	4 1 1 A1	2	8 1 2 A2	9 0.07	1 1
1127.8692	1.5E-23	4 0 3 E	3	16 1 2 E	3 0,62	4 1
1140.1832	2.9E-23	4 2 3 E	1	17 1 2 E	4 --0.10	3 1
1154.3017	5.6E-23	4 1 2 E	3	16 0 2 E	6 -0.29	1 4
1131.3057	2.5E-23	4 1 3 E	4	16 0 2 E	6 -0.16	3 4
1281.1742	2.2E-23	4 2 3 E	1	9 2 2 E	8 0.27	3 2
1319,1190	3.0E-23	4 0 1 E	1	9 0 2 E	9 0.01	2 3
1280.7643	3.7E-23	4 0 3 E	3	9 0 2 E	9 0.25	4 3
1319.2780	2.2E-23	4 1 1 E	2	9 1 2 E	10 0.11	1 2
1280.9530	3.2E-23	4 1 3 E	4	9 1 2 E	10 -0.22	3 2
1267.(943	3.3E-23	2 1 3 E	6	7 1 2 E	11 -0.37	3 2
1432.2144	5.1E-23	4 1 3 E	4	15 0 2 E	15 -0.84	3 1
1128.8087	2.9E-24	3 1 3 E	8	15 0 2 E	15 -0.23	5 1
1420.6973	8.2E-24	4 3 3 E	5	15 2 2 E	17 -0.63	1 1
1319.4059	5.2E-24	3 1 1 E	4	8 1 2 E	20 -0.08	1 2
1319.3725	6.9E-24	3 0 1 E	5	8 0 2 E	21 -0.71	2 3
1436.0484	4.0E-24	3 3 3 E	10	11 2 2 E	25 -0.10	3 2

Figure Caption

Figure 1 FTIR spectrum of CH_3D in the region of the ν_6 Q branch.

footnote: The spectrum was recorded at 0.0056 cm^{-1} resolution with a path of 0.05m and a pressure of 44 *torr* at 293.5 K. The traces are the simulated (top) and observed (middle) spectra, with the observed - calculated residuals in percent (bottom). The scale of the residual plot is ±6%. The synthetic spectrum was calculated using a Voight profile with a self pressure broadening coefficient of 0.09 cm^{-1}/atm. The corresponding line list is reported in Table 5.

Table Captions

Table 1. Vibrational Energies Of the Triad and Nonad of CH_3D.
footnote: The Number quoted in the last column is used to identify the vibrational levels in Tables 5 and 7.

Table 2. Conditions Of the Kitt Peak experiments.

Table 3. Effective Hamiltonian parameters for the Triad of CH_3D.
footnote: All values in cm.

Table 4. Effective Transition Moment Parameters.
footnote: Values in 1 Debye. Five first order parameters were found not significant and then fixed to zero.

Table 5. Sample of the Obs Calc comparison of the IR spectrum of CH_3D.
footnote: The frequency range corresponds to Fig. 1. (a) Observed wavenumber in cm^{-1}; (b) calculated intensity in $cm/molecule$ assuming 100% CH_3D (the intensity threshold is $10^{-25} cm/molecule$); (c) Lower Energy in cm^{-1}; (d) Obs.-Calc. residuals from present work in $10^{-3} cm^{-1}$ (e) Obs.-Calc residuals as reported in (*12*) in $10^{-3} cm^{-1}$ (f) Assignment: V' J K C V" J" K" C" are the quantum numbers for the lower and upper levels respectively: V and V' designate the vibrational levels (refer to Table 1); J and J' are the rotational quantum numbers; K and K" denote the absolute value of the rotational projection quantum number; C and C' designate the symmetry species in the C_{3v} group. "hot" is used to draw attention 011 hot band transitions; * indicates assignment modification with respect to (*12*).

Table 6. Estimated intensity summations of the Nonad Triad System.
footnote: Summations based 011 an intensity threshold of 10^{-25} $cm^{-1}/(molecule.cm^{-2})$ assuming 100% CH_3D. These summations are not accurate indications of the true integrated band strengths.

Table 7. Sample of the Nonad Triad hot transitions.
footnote: (a) Calculated wavenumber in cm^{-1}; (b) Calculated intensity in $cm/molecule$ assuming 100% CH_3D (the intensity threshold is $10^{-25} cm/molecule$); (c) Assignment (see footnote of Table 5); The extra columns N and N' are the running numbers of the levels in increasing order. (d) Averaged discrepancies among transition partners in $10^{-3} cm^{-1}$; (e) i; i': Number of assigned partners involved in the Lower and Upper levels respectively.

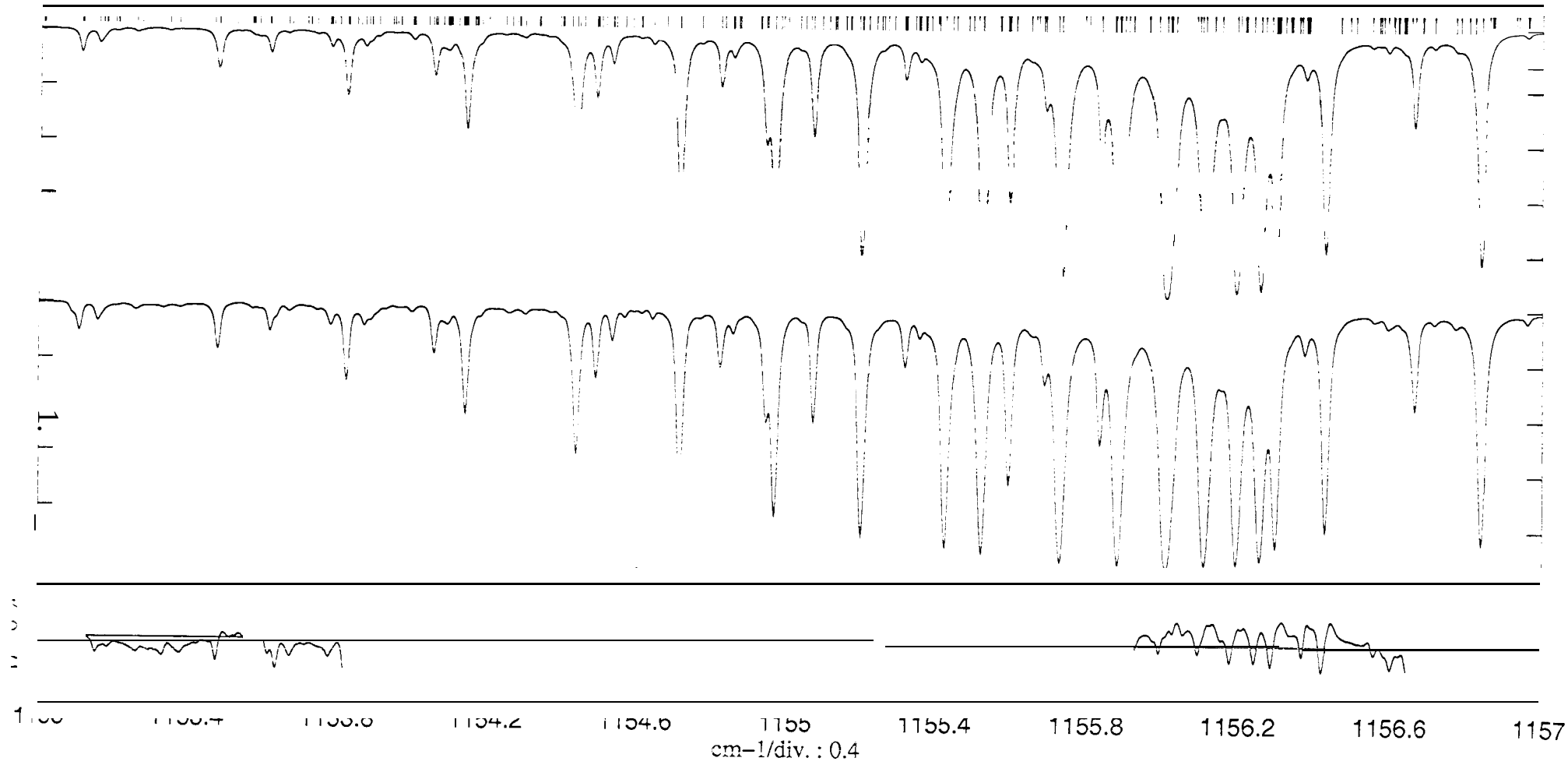
1.
1155.4
1155.8
1156.2
1156.6
1157
cm−1/div. : 0.4